IEEE Access
Multidisciplinary | Rapid Review | Open Access Journal

Received February 21, 2020, accepted March 29, 2020, date of publication April 13, 2020, date of current version May 5, 2020.

Digital Object Identifier 10.1109/ACCESS.2020.2987359

Accelerated Re-Design of Antenna Structures Using Sensitivity-Based Inverse Surrogates

SLAWOMIR KOZIEL[1,2], (Senior Member, IEEE), AND ADRIAN BEKASIEWICZ[2], (Senior Member, IEEE)

[1]School of Applied Engineering, Reykjavik University, Reykjavik 101, Iceland
[2]Faculty of Electronics, Telecommunications and Informatics, Gdansk University of Technology, 80-233 Gdansk, Poland

Corresponding author: Adrian Bekasiewicz (bekasiewicz@ru.is)

This work was supported in part by the Icelandic Centre for Research (RANNIS) under Grant 174573051, and in part by the National Science Centre of Poland under Grant 2017/27/B/ST7/00563.

ABSTRACT The paper proposes a novel framework for accelerated re-design (dimension scaling) of antenna structures using inverse surrogates. The major contribution of the work is a sensitivity-based model identification procedure, which permits a significant reduction of the number of reference designs required to render the surrogate. Rigorous formulation of the approach is supplemented by its comprehensive numerical validation using a triple-band uniplanar dipole antenna and a dual-band monopole antenna re-designed with respect to operating frequencies as well as the substrate parameters (thickness and dielectric permittivity). It is demonstrated that—for the considered test cases—the reliable inverse model can be set up using a significantly smaller (by a factor of three) number of reference points as compared to the original version of the method, whereas the dimension scaling process itself requires up to four EM simulations of the antenna structure.

INDEX TERMS Antenna design, dimension scaling, inverse modeling, simulation-driven design, response sensitivities.

I. INTRODUCTION

Full-wave electromagnetic (EM) analysis has become a mandatory tool in the design of contemporary antenna structures. Meeting stringent performance requirements concerning both electrical and field properties [1]–[7], as well as functionality demands (multi-band operation [8], circular polarization [9], polarization diversity [10], etc.) leads to topologically complex structures that can be neither developed nor optimized using simpler (analytical or equivalent network) models. Yet, EM-driven parameter tuning but also other tasks that require a large number of antenna simulations (uncertainty quantification [11], robust design [12]) may incur considerable computational expenses. Reduction of these costs has been the focus of extensive research, resulting in various methods such as incorporation of adjoints sensitivities into gradient-based optimization procedures [13], expedited optimization using sparse sensitivity updates [14], [15], utilization of machine learning methods (typically in the context of global optimization) [16], or surrogate-assisted frameworks involving both data-driven [17], [18] and physics-based surrogates [19]. The techniques employing a particular structure of the antenna responses have also been proposed (e.g., feature-based optimization [20]).

Re-design of antennas for various operating conditions or material parameters (e.g., dielectric permittivity of the substrate) is a commonly undertaken task. When approached in a brute-force manner, it requires re-optimization of all antenna parameters. As explained in the previous paragraph, it is, in general, a computationally expensive endeavor. The dimension scaling process may be accelerated using design curves [21] that account for the dependence between the operating conditions (e.g., resonant frequencies) and geometry parameter values, or recently suggested inverse surrogates [22]. The efficacy of inverse modeling has been demonstrated for rapid re-design of both microwave [23] and antenna structures [24].

In the case of antennas, the surrogate is normally constructed using the reference designs obtained at the low-fidelity (coarse mesh) EM simulation models. One of practical problems here is that as the number of operating conditions that are handled increase, so is the number of the reference designs needed to ensure uniqueness of the inverse model identification. For example, in [25], a total

The associate editor coordinating the review of this manuscript and approving it for publication was Haiwen Liu.

of 27 reference designs have been employed for addressing dimension scaling of triple-band antennas. In general, the number of such designs grows at a polynomial rate, more specifically, it is proportional to the second power of the number of the considered operating conditions. Clearly, the cost of acquiring such designs may be considerable especially if they are to be generated specifically for the purpose of inverse model construction (rather than available from the previous design work on the same antenna structure).

This paper proposes an alternative approach to antenna re-design using inverse surrogates, where model identification is carried out using both the antenna responses and their sensitivities at the reference designs. Using auxiliary optimization procedures, the antenna Jacobian matrices are employed to obtain sensitivities of geometry parameters with respect to the operating conditions pertinent to the design task at hand. Involving sensitivities results in a dramatic reduction of the number of reference designs required to set up the inverse surrogate which is now linearly dependent on the number of operating conditions to be handled. The operation of the proposed framework is demonstrated using two antenna structures, a triple-band uniplanar dipole and a dual-band monopole antenna, re-designed with respect to the operating conditions and the parameters of the dielectric substrate the radiator is implemented on (relative permittivity and thickness). For the considered test cases, the number reference designs needed to construct the inverse surrogate was reduced by a factor of about three, despite of handling three and four figures of interest, respectively. This led to significant computational savings already at the initial stage of the dimension scaling process. At the same time, antenna re-design can be accomplished at the cost of only three to four EM simulations at the high-fidelity level of description.

The originality and the technical contributions of the work include (i) incorporation of sensitivities into the inverse surrogate model for rapid dimension scaling of antenna structures, (ii) development of a rigorous procedure for low-cost estimation of geometry parameter gradients with respect to the antenna performance figures (required for inverse model identification), (iii) implementation of the sensitivity-based re-design framework which is demonstrably superior over the non-sensitivity versions in terms of a dramatic (by a factor fo three) reduction of the number of reference designs required to set up the surrogate model. This feature is critical for the practical utility of surrogate-assisted dimension scaling procedures because the acquisition of reference designs normally incurs considerable computational expenses for problems involving three or more performance figures. To the best of the authors' knowledge, no comparable frameworks have been presented in the literature thus far.

II. DIMENSION SCALING USING SENSITIVITY-BASED INVERSE SURROGATES

This section introduces the considered dimension scaling procedure. Its keystone is an inverse surrogate model, yielding the values of antenna geometry parameters that correspond to the design optimized w.r.t. the selected combinations of performance figures pertinent to the design task at hand. To reduce the number of reference designs required to set up the surrogate, a novel formulation of the model identification process is proposed, which employs antenna sensitivities. These are available as a by-product of the reference design optimization process. Incorporating the sensitivity data permits a considerable reduction of the surrogate model setup cost as demonstrated in Section III.

A. DESIGN OPTIMALITY. REFERENCE DESIGNS

We distinguish N figures of interest (e.g., operating frequencies of a multi-band antenna, substrate parameters, power split ratio, etc.), denoted as f_k, $k = 1, \ldots, N$. The design is understood to be optimal w.r.t. to f_k, denoted as $\boldsymbol{x}_f^*(f_1,\ldots,f_N)$, if

$$\boldsymbol{x}_f^*(f_1, \ldots, f_N) = \arg\min_{\boldsymbol{x}} U(\boldsymbol{x}; f_1, \ldots, f_N) \tag{1}$$

i.e., it minimizes the functional $U(\boldsymbol{x};f_1,\ldots,f_N)$ that encodes the performance requirements imposed on the device at hand, e.g., centering the operating frequencies at the required values, obtaining a required power split for the structure implemented on the substrate of a particular thickness and/or permittivity. Here, $\boldsymbol{x} = [x_1 \ldots x_n]^T$ is a vector of designable parameters. The subscript f in $\boldsymbol{x}_f^*$ indicates that the design is considered at the level of the high-fidelity (or fine) EM simulation model $\boldsymbol{R}_f(\boldsymbol{x})$ of the structure under design.

The foundation for the dimension scaling procedure are the reference designs pre-optimized for selected vectors of figures of interest $[f_1^{(j)} \ldots f_N^{(j)}]^T$, $j = 1, \ldots, p$, typically uniformly distributed within the ranges of interest where the scaling procedure is supposed to work, i.e., $f_k.min \leq f_k^{(j)} \leq f_k.max$, $k = 1, \ldots, N$. For the sake of computational efficiency, these designs are obtained as in (1) at the level of the low-fidelity (or coarse) EM simulation model $\boldsymbol{R}_c(\boldsymbol{x})$, and denoted as $\boldsymbol{x}_c^*(j)$. Additionally, a pair of reference designs $\boldsymbol{x}_f^{*(0)}$ and $\boldsymbol{x}_c^{*(0)}$ is obtained for both the high- and low-fidelity model at an additional figure of interest vector $[f_1^{(0)} \ldots f_N^{(0)}]^T$, typically allocated at or around the center of the interval $[f_{1.\min}, f_{1.\max}] \times \ldots \times [f_N.\min, f_N.\max]$.

For all reference designs, the antenna responses $\boldsymbol{R}_c(\boldsymbol{x}_c^{(j)})$ and the corresponding Jacobian matrices $\boldsymbol{J}_c(\boldsymbol{x}_c^{(j)})$ are known from the process of solving (1).

B. INVERSE SURROGATE MODEL

The re-design process involves an inverse surrogate model that maps the figures of interest f_k into the antenna parameter space. The analytical formulation of the surrogate should account for the typical relationships between f_k and $\boldsymbol{x}$. Here, we adopt the form utilized in [25], where the model $\boldsymbol{s}_c(f_1,f_2,\ldots,f_N)$ is set up independently for each geometry parameter as

$$\boldsymbol{s}_c(f_1, f_2, \ldots, f_N, \boldsymbol{P}) = [s_{c.1}(f_1, f_2, \ldots, f_N, \boldsymbol{p}_1) \quad \ldots \quad s_{c.n}(f_1, f_2, \ldots, f_N, \boldsymbol{p}_n)]^T \tag{2}$$

with $s_{c.l}(f_1, f_2, \ldots f_N, \boldsymbol{p}_l)$ being a model of the lth geometry parameter; $\boldsymbol{p}_l$ stands for the model coefficients. The vector $\boldsymbol{P} = [\boldsymbol{p}_1 \ldots \boldsymbol{p}_n]$ represents the aggregated vector of parameters.

The assumed analytical form of the inverse surrogate is

$$s_{c.l}(f_1, f_2, \ldots, f_N) = q_l(f_1, f_2, \ldots, f_N) \prod_{k=1}^{N} s_{fk.l}(f_k) \quad (3)$$

with

$$s_{fk.l}(f_k) = a_{3k-2.l} + a_{3k-1.l} \exp(a_{3k.l} f_k) \quad (4)$$

for $k = 1, 2, \ldots, N$, and

$$q_l(f_1, f_2, \ldots, f_N) = \lambda_0 + \sum_{k=1}^{N} \lambda_k f_k + \sum_{k=1}^{N} \sum_{j=k+1}^{N} \lambda_{kj} f_k f_j \quad (5)$$

The exponential terms (4) account for the effects of individual figures of interest, whereas their joint effects are modeled by the polynomial term (5).

According to [24], the model parameters are identified by solving the nonlinear regression problem of the form

$$\boldsymbol{p}_l = \arg\min_{\boldsymbol{p}} \sum_{j=1}^{p} \left[s_{c.l}(f_1^{(j)}, \ldots, f_N^{(j)}, \boldsymbol{p}) - x_{c.l}^{(j)} \right]^2 \quad (6)$$

where $\boldsymbol{x}_c^*(j) = [x_{c.}1^{(j)} \ldots x_{c.n}^{(j)}]^T$ is the low-fidelity reference design corresponding to the figures of interest $[f_1^{(j)} \ldots f_N^{(j)}]^T$.

Note that the overall number of parameters is

$$N_P = 3N + (N+1)(N+2)/2 = (N^2 + 9N + 2)/2 \quad (7)$$

which is 6, 12, 19, 27, and 36 for $N = 1, 2, 3, 4$, and 5, respectively. The number of reference designs p should be larger than N_P, not only to ensure uniqueness of model identification but also to smoothen out possible irregularities (e.g., due to imperfect reference design extraction through (1)). Having the inverse surrogate, the re-design process is fast, i.e., only requires a handful of EM simulations of the structure (cf. Section 3); however, identification of a large number of reference designs may incur considerable computational expenses. Reducing the number of required designs is therefore highly desirable.

C. SENSITIVITY-BASED MODEL IDENTIFICATION

The major contribution of this paper is an alternative inverse surrogate identification procedure which aims at reducing the number of reference designs by employing both the antenna responses $\boldsymbol{R}_c(\boldsymbol{x}_c^*(j))$ and the corresponding Jacobians $\boldsymbol{J}_c(\boldsymbol{x}_c^*(j))$ at the reference designs.

The proposed model identification procedure is defined as

$$\boldsymbol{p}_l = \arg\min_{\boldsymbol{p}} \left\{ \sum_{j=1}^{p} \left[s_{c.l}(f_1^{(j)}, \ldots, f_N^{(j)}, \boldsymbol{p}) - x_{c.l}^{(j)} \right]^2 + \frac{1}{N} \sum_{j=1}^{p} \sum_{k=1}^{N} \left[\frac{\partial s_{c.l}(f_1^{(j)}, \ldots, f_N^{(j)}, \boldsymbol{p})}{\partial f_k} - J_{lk}^x(x_{c.l}^{(j)}) \right]^2 \right\} \quad (8)$$

where $\partial s_{c.l}/\partial f_k$ are partial derivatives of the inverse surrogate (3) w.r.t. the figures of interest, whereas $J_{lk}^x(\cdot)$ are the components of the Jacobian matrix $\boldsymbol{J}^x$ containing partial derivatives of the reference design components w.r.t. to f_k. The normalization factor $1/N$ is introduced to balance the contribution of the reference design coordinates and their sensitivities to the functional under minimization. Identifying the surrogate according to (8) yields the best possible alignment (in the L-square sense) between the model and the reference designs both in terms of the values and their sensitivities. Note that (8) imposes $N+1$ conditions on the surrogate per reference design, therefore the minimum number of the reference points that ensure uniqueness of the extraction process is

$$N_P = \left\lceil \frac{N^2 + 9N + 2}{2(N+1)} \right\rceil \quad (9)$$

where $\lceil \cdot \rceil$ is the ceiling function. Thus, for $N = 1, 2, 3, 4$, and 5 we now have $N_P = 3, 4, 5, 6$, and 6, respectively. The potential savings as compared to (7) are evident.

What remains to be addressed is a procedure for obtaining the partial derivatives $\partial s_{c.l}/\partial f_k$ (these can be found analytically from (3)), and the Jacobian matrix $\boldsymbol{J}^x$, which is slightly more complicated. For the latter, let $\boldsymbol{d} = [d_1 \ldots d_N]^T$ be a vector of perturbations of the performance figures. In the first step, we find the perturbed reference designs $\boldsymbol{x}_c^{*(j.k)}$ corresponding to vectors $[f_1^{(j)} \ldots f_k^{(j)} + d_k \ldots f_N^{(j)}]^T$,

$$\boldsymbol{x}_c^{*(j.k)} = \arg\min_{\boldsymbol{x}} U_L(\boldsymbol{x}; f_1^{(j)}, \ldots, f_k^{(j)} + d_k, f_N^{(j)}) \quad (10)$$

in which the objective function U_L is based on the first-order expansion of $\boldsymbol{R}_c$

$$\boldsymbol{R}_c(\boldsymbol{x}) = \boldsymbol{R}_c(\boldsymbol{x}_c^{*(j)}) + \boldsymbol{J}_c(\boldsymbol{x}_c^{*(j)}) \cdot (\boldsymbol{x} - \boldsymbol{x}_c^{*(j)}) \quad (11)$$

rather than $\boldsymbol{R}_c$ itself (cf. (1)). This ensures that the cost of solving (10) is negligible. The actual values of the figures interest $[f_1^{(j.k)} \ldots f_N^{(j.k)}]^T$, corresponding to $\boldsymbol{x}_c^{*(j.k)}$ are then extracted from $\boldsymbol{R}_c$ $(\boldsymbol{x}_c^{*(j.k)})$ which requires just one EM simulation at the low-fidelity level of accuracy. As mentioned above, the Jacobians $\boldsymbol{J}_c(\boldsymbol{x}_c^*(j))$ are known beforehand. Given that the perturbations d_k are small (their particular values are not critical), we have

$$x_{c.l}^{*(j.k)} \approx x_{c.l}^{*(j)} + \sum_{r=1}^{N} J_{lr}^x(\boldsymbol{x}_c^{*(j)})[f_r^{(j.k)} - f_r^{(j)}] \quad (12)$$

One can rewrite (12) in the matrix form as follows

$$\boldsymbol{X} = \boldsymbol{J}^x \boldsymbol{F} \quad (13)$$

where

$$\boldsymbol{X} = \left[\boldsymbol{x}_c^{*(j.1)} - \boldsymbol{x}_c^{*(j)} \quad \cdots \quad \boldsymbol{x}_c^{*(j.N)} - \boldsymbol{x}_c^{*(j)} \right] \quad (14)$$

and

$$\boldsymbol{F} = \begin{bmatrix} f_1^{(j.1)} - f_1^{(j)} & \cdots & f_1^{(j.N)} - f_1^{(j.N)} \\ \vdots & \ddots & \vdots \\ f_N^{(j.1)} - f_N^{(j)} & \cdots & f_N^{(j.N)} - f_N^{(j.N)} \end{bmatrix} \quad (15)$$

If the matrix $\boldsymbol{F}$ is invertible, equation (13) has a solution

$$\boldsymbol{J}^x = \boldsymbol{X}\boldsymbol{F}^{-1} \tag{16}$$

Note that in the special (ideal) case when $[f_1^{(j.k)} \ldots f_N^{(j.k)}]^T = [f_1^{(j)} \ldots f_k^{(j)} + d_k \ldots f_N^{(j)}]^T$, the matrix $\boldsymbol{F}$ is diagonal of the form $\boldsymbol{F} = \text{diag}(d_1,\ldots,d_N)$. In practice, even though $[f_1^{(j.k)} \ldots f_N^{(j.k)}]^T \neq [f_1^{(j)} \ldots f_k^{(j)} + d_k \ldots f_N^{(j)}]^T$, off-diagonal elements are small, therefore non-singularity of $\boldsymbol{F}$ normally holds. Again, in the aforementioned special case, we have

$$x_{c.l}^{*(j.k)} \approx x_{c.l}^{*(j)} + J_{lk}^x(\boldsymbol{x}_c^{*(j)})d_k \tag{17}$$

which implies

$$J_{lk}^x(\boldsymbol{x}_c^{*(j)}) \approx \left[x_{c.l}^{*(j.k)} - x_{c.l}^{*(j)}\right]/d_k \tag{18}$$

Then, as $\boldsymbol{F} = \text{diag}(d_1,\ldots,d_N)$, (16) coincides with (18).

D. SCALING PROCEDURE

The inverse surrogate outputs the geometry parameter values corresponding to (nearly optimum) design scaled do the target values of figures of interest f_1 through f_N. As the surrogate is constructed using the low-fidelity EM data, a correction has to be made to account for the discrepancies between the low- and high-fidelity EM models. The basic scaling procedure is implemented as [24]:

$$\boldsymbol{x}_f(f_1, f_2, \ldots, f_N) = \boldsymbol{s}_c(f_1, f_2, \ldots, f_N, \boldsymbol{P}) + \left[\boldsymbol{x}_f^{*(0)} - \boldsymbol{x}_c^{*(0)}\right] \tag{19}$$

where $\boldsymbol{x}_f^{*(0)}$ and $\boldsymbol{x}_c^{*(0)}$ are the additional high- and low-fidelity reference design corresponding to $[f_1^{(0)} \ldots f_N^{(0)}]^T$ (cf. Section 2.1).

Due to non-perfect correlations between $\boldsymbol{R}_c$ and $\boldsymbol{R}_f$, the scaling (19) leads to certain errors which can be corrected by a simple iterative procedure of the form [25]

$$\boldsymbol{x}_f^{(i+1)}(f_1, f_2, \ldots, f_N) = \boldsymbol{s}_c(f_1 - \sum_{k=1}^{i} \Delta f_{1.k}, \ldots, f_N - \sum_{k=1}^{i} \Delta f_{N.k}, \boldsymbol{P}) + \left[\boldsymbol{x}_f^{*(0)} - \boldsymbol{x}_c^{*(0)}\right] \tag{20}$$

Here, $\boldsymbol{x}_f^{(i)}$ is the high-fidelity antenna design at the ith iteration of the correction process ($\boldsymbol{x}_f^{(0)}$ being the design obtained from (19)); $\Delta f_j.k$ is the error of the jth figure of interest frequency at the kth iteration. Note that (20) employs the accumulated scaling errors $\sum_k = 1, \ldots, i\Delta f_{j.k}$. This is to account for the fact that the new corrected design $\boldsymbol{x}_f^{(i+1)}$ is a "shift" w.r.t. $\boldsymbol{x}_f(i)$. The computational cost of each iteration (20) is only one high-fidelity EM analysis. Furthermore, the procedure quickly converges (in practice, three or four iterations are required). Figure 1 shows the flow diagram of the entire re-design procedure.

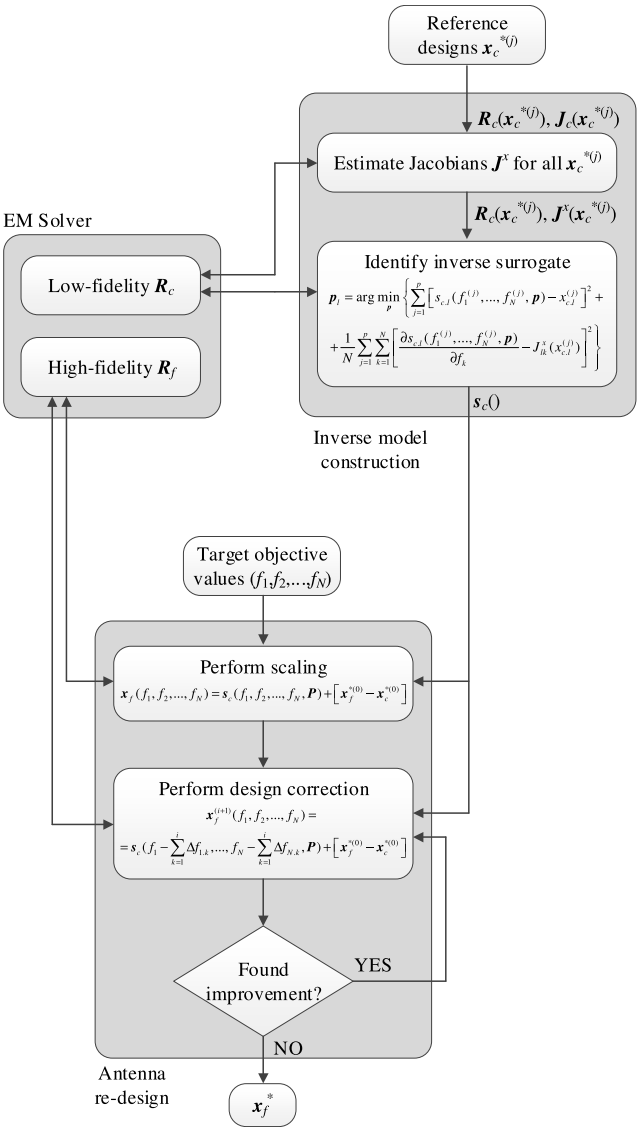

FIGURE 1. Flow diagram of the sensitivity-based dimension scaling framework. The top part refers to the construction of the sensitivity-based inverse surrogate model, whereas the bottom part illustrates the flow of the re-design procedure, which consists of the initial dimension scaling and the iterative correction process, where the accumulated scaling errors are employed to accommodate over- or under-shooting of the figures of interest (in Section 3, the operating frequencies of the antenna structures under design).

III. VERIFICATION CASE STUDIES

In this section, the proposed sensitivity-based dimension scaling procedure is validated using two antenna structures: (i) a triple-band uniplanar dipole antenna re-designed with respect to the target operating frequencies, and (ii) a dual-band monopole antenna re-designed with respect to the operating frequencies, as well as the substrate permittivity and thickness. Both problems are challenging due to several performance figures that need to be accounted for. The presented approach is compared to the non-sensitivity-based approach.

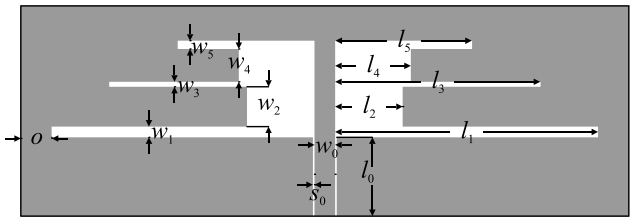

FIGURE 2. Geometry of the triple-band dipole antenna [25].

A. EXAMPLE 1: TRIPLE-BAND UNIPLANAR DIPOLE ANTENNA

The first test case is a triple-band uniplanar dipole antenna shown in Fig. 2. The structure is based on the design presented in [26]. It is implemented on a Taconic RF-35 substrate ($h = 0.762$ mm, $\tan\delta = 0.0018$, $\varepsilon_r = 3.5$). The antenna is fed through a 50 ohm coplanar waveguide (CPW). The design variables are $\boldsymbol{x} = [l_1 l_2 l_3 \ l_4 l_5 w_1 w_2 \ w_3 w_4 w_5]^T$. Parameters $l_0 = 30$, $w_0 = 3$, $s_0 = 0.15$ and $o = 5$ are fixed (all dimensions in mm). The radiator computational models are implemented in CST Microwave Studio and evaluated using its time-domain solver [27]. The high-fidelity model $\boldsymbol{R}_f$ contains about 550,000 mesh cells and its simulation time on dual Intel Xeon E5540 machine with 64 GB RAM is about 3 minutes. The low-fidelity model $\boldsymbol{R}_c$ contains about 97,000 cells (simulation time 23 seconds).

The objective is to re-design the antenna to allocate the resonances at the target frequencies f_1, f_2, and f_3 within the following ranges thereof: 1.5 GHz $\leq f_1 \leq$ 2.5 GHz, $f_2 = k_1 f_1$ and $f_3 = k_2 f_2$, $1.2 \leq k_1, k_2 \leq 1.6$. This example has been considered in [25] and re-designed using the non-sensitivity based inverse surrogates (cf. (2)-(6)). Therein, 27 reference design were used, which corresponded to all combinations of the operating frequencies $f_1 \in \{1.5, 2.0, 2.5\}$ GHz, and $f_2 = k_1 f_1$, $f_3 = k_1 k_2 f_1$ with $k_1, k_2 \in \{1.2, 1.4, 1.6\}$. Additionally, a single high-fidelity model reference design was used, corresponding to $f_1 = 2.0$ GHz, $k_1 = k_2 = 1.4$, $\boldsymbol{x}_f^*(2.0,2.8,3.92) = [38.2\ 9.6\ 31.7\ 9.8\ 22.5\ 0.35\ 2.8\ 0.75\ 1.30\ 0.20]^T$ mm.

The corresponding low-fidelity reference design is $\boldsymbol{x}_c^*(2.0,2.8,3.92) = [36.7\ 9.2\ 32.6\ 8.8\ 22.8\ 0.41\ 1.52\ 0.85\ 1.48\ 0.22]^T$ mm. The reference designs have been optimized using the feature-based optimization technique [20] with the optimization cost being a few dozen of low-fidelity EM model evaluations per design.

Note that given three figures of interest, the minimum number of reference designs is 19 (cf. (7)), and, as mentioned before, the actual number should be higher in order to smoothen out possible irregularities due to imperfect optimization of the reference designs, etc. According to (9), the minimum number of reference designs for sensitivity-based inverse surrogate is five. Here, we use nine points, corresponding to the corners of the objective space, i.e., $\{f_1, k_1, k_2\} = \{1.5, 1.2, 1.2\}, \{1.5, 1.2, 1.6\}, \{1.5, 1.6, 1.2\}, \{1.5, 1.6, 1.6\}, \{2.5, 1.2, 1.2\}, \{2.5, 1.2, 1.6\}, \{2.5, 1.6, 1.2\}, \{2.5, 1.6, 1.6\}$, and the center $\{2.0, 1.4, 1.4\}$.

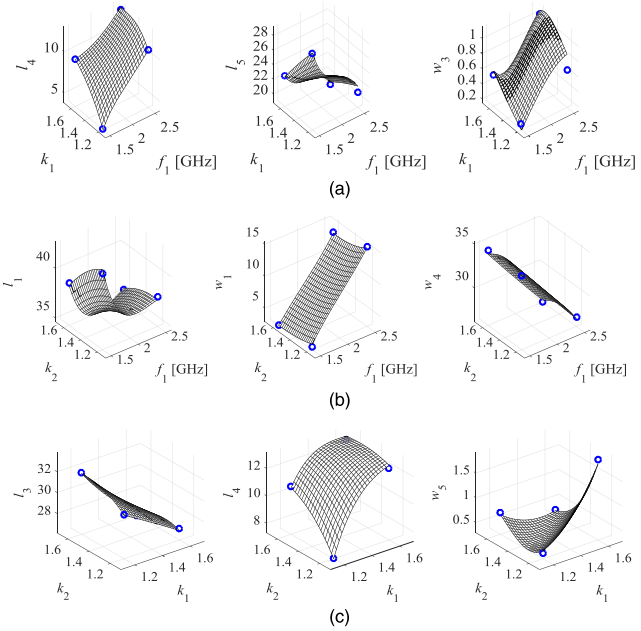

FIGURE 3. Triple-band dipole antenna: selected two-dimensional cuts of the sensitivity-based inverse surrogate model for selected geometry parameters: (a) f_1 - k_1 plane, (b) f_1 - k_2 plane, and (c) k_1 - k_2 plane. Reference designs marked using circles.

The selected two-dimensional cuts of the inverse surrogate obtained using (8) have been shown in Fig. 3. Because the surrogate is constructed using limited information from the reference designs, dimension scaling errors are unavoidable. However, it can be observed that the surrogate adequately represents the trends between the figures of interest and the reference designs. In particular, the monotonicity relationships between the antenna geometry parameters and the operating frequencies seem to be well preserved. This is an indication that the correction procedure (20) is likely to work well.

Verification of the scaling procedure of Section 2 has been carried out by re-designing the antenna for the following six sets of target operating frequencies: $[f_1\ f_2\ f_3] = [1.6\ 2.1\ 3.2]$ GHz, $[f_1\ f_2\ f_3] = [1.6\ 2.45\ 3.1]$ GHz, $[f_1\ f_2\ f_3] = [1.8\ 2.45\ 3.6]$ GHz, $[f_1\ f_2\ f_3] = [1.8\ 2.7\ 4.1]$ GHz, $[f_1\ f_2\ f_3] = [2.4\ 3.5\ 4.5]$ GHz, and $[f_1\ f_2\ f_3] = [2.4\ 3.8\ 5.8]$ GHz.

The reflection responses corresponding to the final designs obtained using the procedure of Section 2 with sensitivity-based inverse surrogates can be found in Fig. 4. Note that the initial scaling errors are quite considerable as expected; however, all designs are well aligned with the required operating frequencies upon accomplishing the correction stage (cf. (20)). The antenna matching is also good in all instances. The average cost of the correction procedure was three iterations (i.e., three EM simulations of the antenna structure). The specific antenna dimensions have been gathered in Table 1.

For the sake of comparison, the antenna was re-designed using the non-sensitivity-based inverse surrogates [25]. It can be observed, also in Fig. 4, that the design quality is comparable for both methods. However, as mentioned before,

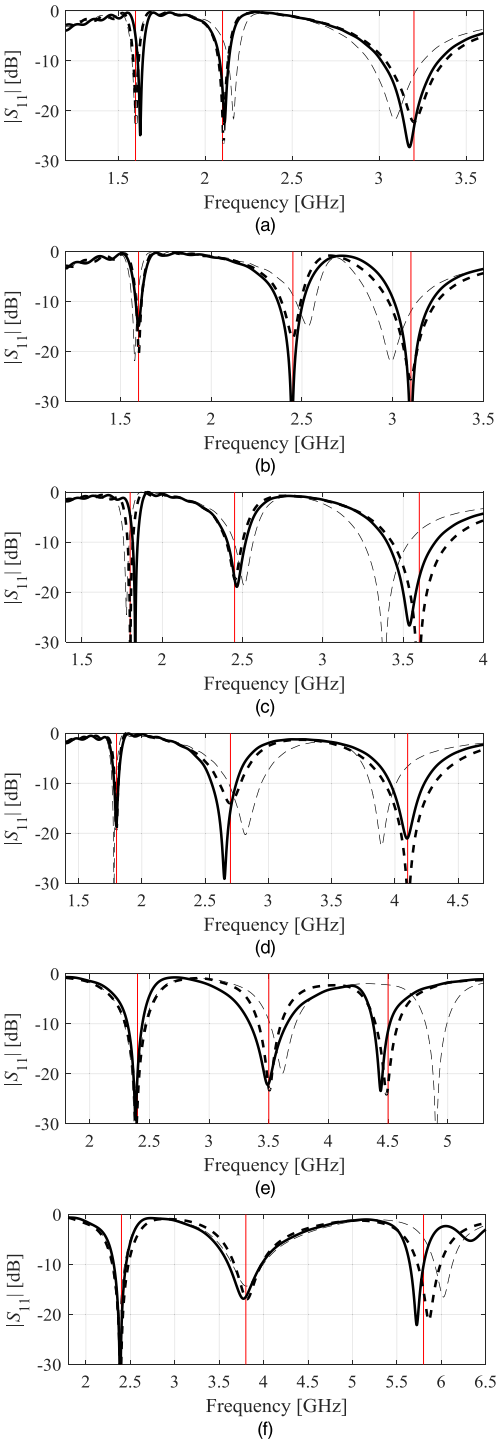

FIGURE 4. Verification results: triple-band dipole antenna scaled for: (a) $[f_1\ f_2\ f_3] = [1.6\ 2.1\ 3.2]$ GHz, (b) $[f_1\ f_2\ f_3] = [1.6\ 2.45\ 3.1]$ GHz, (c) $[f_1\ f_2\ f_3] = [1.8\ 2.45\ 3.6]$ GHz, (d) $[f_1\ f_2\ f_3] = [1.8\ 2.7\ 4.1]$ GHz, (e) $[f_1\ f_2\ f_3] = [2.4\ 3.5\ 4.5]$ GHz, (f) $[f_1\ f_2\ f_3] = [2.4\ 3.8\ 5.8]$ GHz. Responses before correction (20) of Section 2.4, i.e., obtained from the sensitivity-based inverse surrogate marked using thin dashed line; the final designs obtained using the sensitivity- and non-sensitivity-based technique (benchmark) marked using thick solid and dashed lines, respectively. Required operating frequencies are marked using vertical lines.

the non-sensitivity-based approach required 27 reference designs. Thus, the computational benefits of the proposed methodology are evident.

TABLE 1. Dimensions of the triple-band antenna at verification designs.

No.	Operating Frequencies [GHz]			Geometry Parameters [mm]								
	f_1	f_2	f_3	l_1	l_2	l_3	l_4	l_5	w_1	w_2	w_3	w_4	w_5
1	1.6	2.1	3.2	39.8	5.13	33.6	6.18	26.0	0.20	1.23	0.21	3.11	0.69
2	1.6	2.45	3.1	42.4	4.93	33.8	9.04	26.2	0.42	3.03	0.63	1.57	0.20
3	1.8	2.45	3.6	37.9	7.48	32.4	8.27	23.8	0.20	2.38	0.44	2.54	0.67
4	1.8	2.7	4.1	37.6	5.80	31.9	9.93	21.8	0.20	2.40	0.23	2.33	0.30
5	2.4	3.5	4.5	37.8	14.1	28.6	11.4	22.4	0.44	2.23	1.45	0.20	0.46
6	2.4	3.8	5.8	37.9	14.3	27.0	13.3	21.2	0.27	2.42	1.18	0.31	0.37

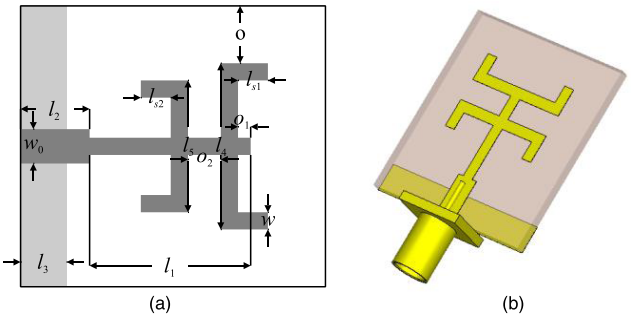

FIGURE 5. A dual-band antenna with two C-shaped radiating strips: (a) geometry with highlighted design parameters and (b) visualization of the antenna high-fidelity model.

B. EXAMPLE 2: TRIPLE-BAND UNIPLANAR DIPOLE ANTENNA

As the second example, consider a dual-band monopole antenna shown in Fig. 5. The structure is based on the radiator of [28]. It consists of a driven element in the form of two C-shaped structures interconnected by a central strip and fed through a stepped impedance microstrip line. The vector of geometry parameters is $\boldsymbol{x} = [l_1\ l_2\ l_3\ l_4\ l_5\ w\ o_1 r\ o_2 r]^T$. The relative variables are $o_1 = (0.5l_1 - w)o_1 r$, $o_2 = o_1 + w + (l_1 - o_1 - w)o_2 r$, $l_s1 = 0.2(l_4 + 2w)$, $l_s2 = 0.2(l_5 + 2w)$, whereas $o = 5$ remains fixed. Parameter w_0 is calculated based on the transmission line theory for the given values of substrate permittivity ε_r and thickness h [24]. The unit for all geometry parameters (except the ones with r in subscript) is mm. Geometrical consistency of the antenna model is maintained for the following lower and upper bounds: $\boldsymbol{l} = [15\ 5\ 3\ 10\ 10\ 0.5\ 0.1\ 0.1]^T$ and $\boldsymbol{u} = [25\ 10\ 10\ 20\ 20\ 3\ 0.9\ 0.9]^T$.

The computational model of the structure is implemented in CST Microwave Studio and evaluated using its time-domain solver [27]. The low-fidelity model $\boldsymbol{R}_c$ is discretized using ∼200,000 hexahedral mesh cells and its average simulation time on a dual Intel Xeon E5540 machine with 64 GB RAM is 52 s. The high-fidelity model $\boldsymbol{R}_f$ comprises ∼900,000 cells and its typical simulation time is 170 s. Besides relaxed mesh density, other simplifications incorporated in $\boldsymbol{R}_c$ include representing metallization as perfect electrical conductor and the lack of the SMA connector.

The objective is to re-design the antenna with respect to four figures of interest: the operating frequencies f_1 and f_2, as well as permittivity and height of the substrate the radiator is implemented on. The scaling procedure is supposed to work within the following ranges: 2.0 GHz $\leq f_1 \leq$ 3.0 GHz, 5.0 GHz $\leq f_2 \leq$ 6.0 GHz, 2.5 $\leq \varepsilon_r \leq$ 4.5, and 0.6 mm $\leq h \leq$ 1.6 mm.

The sensitivity-based inverse surrogate is set up using 17 reference designs corresponding to the corners of the aforementioned objective space, i.e., $\{f_1, f_2, \varepsilon_r, h\} = \{2.0, 5.0, 2.5, 0.6\}$, $\{2.0, 5.0, 2.5, 1.6\}$, $\{2.0, 5.0, 4.5, 0.6\}$, …, $\{3.0, 6.0, 4.5, 1.6\}$ as well as the its center, i.e., $\{f_1, f_2, \varepsilon_r, h\} = \{2.5, 5.5, 3.5, 1.1\}$. Additionally, a single high-fidelity model reference design was used, also corresponding to $\{f_1, f_2, \varepsilon_r, h\} = \{2.5, 5.5, 3.5, 1.1\}$, $\boldsymbol{x}_f^*$(2.5,5.5,3.5,1.1) = $[27.0\ 5.62\ 4.74\ 1.00\ 1.35\ 2.87\ 0.30\ 0.46]^T$. The corresponding low-fidelity reference design is $\boldsymbol{x}_c^*$(2.5,5.5,3.5,1.1) = $[23.7\ 7.67\ 5.05\ 2.69\ 3.04\ 2.68\ 0.45\ 0.28]^T$ mm. As for the first example, the reference designs have been found using feature-based optimization [20] with the optimization cost being a few dozen of low-fidelity EM model evaluations per design.

It should be emphasized that given four figures of interest, the minimum number of reference designs is 27 (cf. (7)), for the non-sensitivity-based technique. Here, for the sake of comparative experiments the non-sensitivity-based inverse surrogate has been constructed sing 50 reference points, which include the seventeen points employed by the proposed method as well as 33 additional points corresponding to randomly allocated values of the figures of interest. According to (9), the minimum number of reference designs for sensitivity-based inverse surrogate is only six. The reason for using 17 designs is to include all corners of the objective space, which still gives a significant computational savings (by a factor of three).

Figure 6 show the selected two-dimensional cuts of the inverse surrogate obtained using (8). Similarly as in Section 3.1, although the accuracy of the surrogate is limited, it is expected that the iterative correction (20) will work properly given appropriate account for the overall relationships between the figures of interest and geometry parameters.

Verification of the scaling procedure of Section 2 has been carried out by re-designing the antenna for the following six sets of target operating frequencies: [f_1 f_2 ε_r h] = [2.2 5.1 2.5 0.76], [2.45 5.5 2.5 0.76], [2.2 5.1 3.5 0.81], [2.45 5.3 3.5 1.0], [2.7 5.8 4.4 1.0], and [2.7 5.8 2.5 1.0] (frequency in GHz, substrate height in mm).

Figure 7 shows the reflection responses corresponding to the final designs obtained using the procedure of Section 2 with sensitivity-based inverse surrogates. In this case, the initial scaling errors are not as significant as for the previous example, and the antenna resonances are well aligned with the target operating frequencies upon accomplishing the correction stage (cf. (20). The cost of the correction procedure was three iterations (i.e., three EM simulations

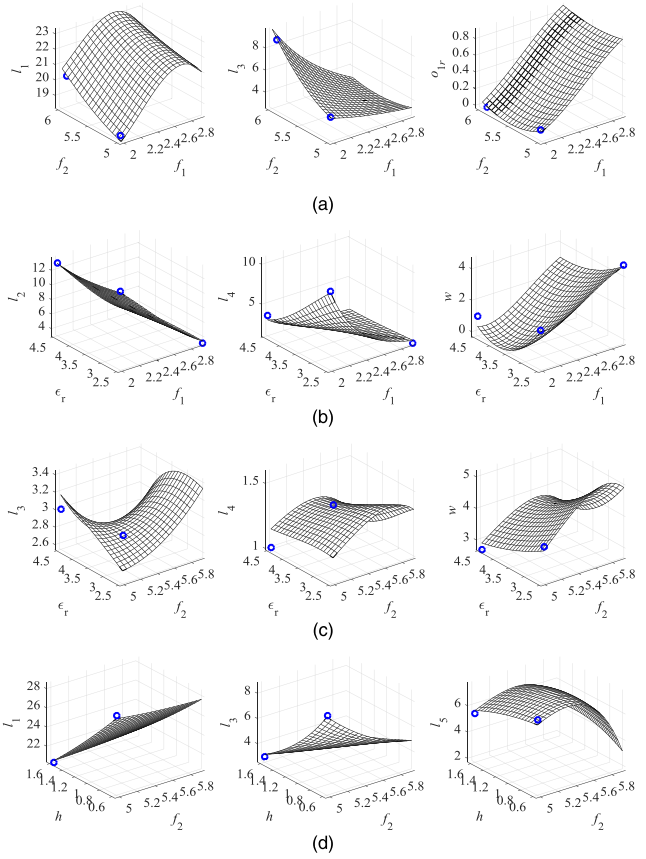

FIGURE 6. Dual-band monopole antenna: selected two-dimensional cuts of the sensitivity-based inverse surrogate model for selected geometry parameters: (a) f_1 - f_2 plane, (b) f_1 - ε_r plane, (c) f_2 - ε_r plane, and (d) f_2 - h plane. Reference designs marked using circles.

TABLE 2. Dimensions of the dual-band antenna at verification designs

No.	Figures of Interest [GHz]		N/A [mm]		Geometry Parameters [mm]							
	f_1	f_2	ε_r	h	l_1	l_2	l_3	l_4	l_5	w	o_{1r}	o_{1r}
1	2.2	5.1	2.5	0.76	25.4	9.43	5.52	2.85	1.50	2.75	0.03	0.50
2	2.45	5.5	2.5	0.76	26.2	6.91	4.77	1.33	1.50	2.88	0.45	0.50
3	2.2	5.1	3.5	0.81	28.2	8.34	5.44	1.60	1.64	1.82	0.09	0.46
4	2.45	5.3	3.5	1.0	27.7	5.56	4.55	0.94	2.05	2.84	0.36	0.49
5	2.7	5.8	4.4	1.0	27.9	2.00	3.58	0.80	1.50	2.16	0.86	0.29
6	2.7	5.8	2.5	1.0	26.0	4.84	4.09	0.87	1.50	3.94	0.51	0.47

of the antenna structure). Table 2 provides the antenna dimensions.

As a benchmark, the antenna was re-designed using the non-sensitivity-based inverse surrogates [25]. Figure 7 indicates that the design quality is comparable for both methods. Notwithstanding, the non-sensitivity-based approach was executed using 50 reference designs, whereas the proposed approach only required 17 reference points. Thus, the cost of setting up the inverse surrogate has been reduced by a factor of three.

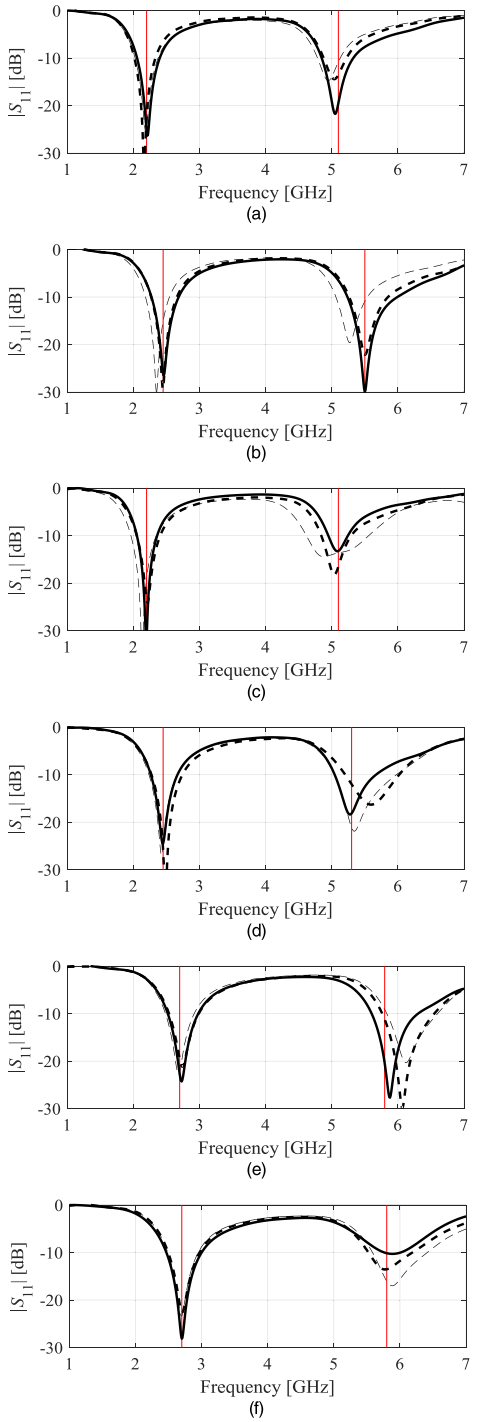

FIGURE 7. Verification results: dual-band antenna scaled for: (a) [f_1 f_2 ε_r h] = [2.2 5.1 2.5 0.76], (b) [f_1 f_2 ε_r h] = [2.45 5.5 2.5 0.76], (c) [f_1 f_2 ε_r h] = [2.2 5.1 3.5 0.81], (d) [f_1 f_2 ε_r h] = [2.45 5.3 3.5 1.0], (e) [f_1 f_2 ε_r h] = [2.7 5.8 4.4 1.0], (f) [f_1 f_2 ε_r h] = [2.7 5.8 2.5 1.0]. Responses before correction (20) of Section 2.4, i.e., obtained from the sensitivity-based inverse surrogate marked using thin dashed line; the final designs obtained using the sensitivity- and non-sensitivity-based technique (benchmark) marked using thick solid and dashed lines, respectively. Required operating frequencies are marked using vertical lines.

IV. CONCLUSION

In the paper, a novel framework for fast dimension scaling of antenna structures has been proposed. Its major contribution is a sensitivity-based procedure for inverse surrogate model identification, which allows for a significant (by up to seventy percent) reduction of the number of reference designs required to render the model. This facilitates handling more challenging design situations that involve three or more figures of interest simultaneously. The surrogate modeling process is rigorously formulated including the low-cost algorithm for extracting the geometry parameter sensitivities with respect to the relevant performance figures. Our methodology is comprehensively validated using a triple-band dipole antenna re-designed with respect to the operating frequencies and a dual-band patch antenna re-designed for operating frequencies and substrate parameters. Here, the inverse surrogates are constructed using only nine and seventeen reference designs, respectively, despite handling three and four performance figures. The models yield accurate predictions, further improved using the iterative correction process. Comparison with the non-sensitivity based inverse models indicates that reduction of the number of reference designs does not lead to any degradation of the results quality.

REFERENCES

[1] N. Nguyen-Trong and C. Fumeaux, "Tuning range and efficiency optimization of a frequency-reconfigurable patch antenna," *IEEE Antennas Wireless Propag. Lett.*, vol. 17, no. 1, pp. 150–154, Jan. 2018.

[2] A. A. Omar and Z. Shen, "A compact and wideband vertically polarized monopole antenna," *IEEE Trans. Antennas Propag.*, vol. 67, no. 1, pp. 626–631, Jan. 2019.

[3] Y.-S. Chen and Y.-H. Chiu, "Application of multiobjective topology optimization to miniature ultrawideband antennas with enhanced pulse preservation," *IEEE Antennas Wireless Propag. Lett.*, vol. 15, pp. 842–845, 2016.

[4] R. Bhattacharya, R. Garg, and T. K. Bhattacharyya, "Design of a PIFA-driven compact yagi-type pattern diversity antenna for handheld devices," *IEEE Antennas Wireless Propag. Lett.*, vol. 15, pp. 255–258, 2016.

[5] A. Lalbakhsh, M. U. Afzal, and K. P. Esselle, "Multiobjective particle swarm optimization to design a time-delay equalizer metasurface for an electromagnetic band-gap resonator antenna," *IEEE Antennas Wireless Propag. Lett.*, vol. 16, pp. 912–915, 2017.

[6] J. Yun, J. Y. Park, and K. C. Hwang, "Optimization of a subarray structure to improve the G/T of an active array antenna," *IEEE Antennas Wireless Propag. Lett.*, vol. 18, no. 10, pp. 2214–2218, Oct. 2019.

[7] M. Kovaleva, D. Bulger, B. A. Zeb, and K. P. Esselle, "Cross-entropy method for electromagnetic optimization with constraints and mixed variables," *IEEE Trans. Antennas Propag.*, vol. 65, no. 10, pp. 5532–5540, Oct. 2017.

[8] C. Goswami, R. Ghatak, and D. R. Poddar, "Multi-band bisected Hilbert monopole antenna loaded with multiple subwavelength split-ring resonators," *IET Microw., Antennas Propag.*, vol. 12, no. 10, pp. 1719–1727, Aug. 2018.

[9] D. Feng, H. Zhai, L. Xi, S. Yang, K. Zhang, and D. Yang, "A broadband low-profile circular-polarized antenna on an AMC reflector," *IEEE Ant. Wireless Prop. Lett.*, vol. 16, pp. 2840–2843, 2017.

[10] G. Wolosinski, V. Fusco, U. Naeem, and P. Rulikowski, "Pre-matched eigenmode antenna with polarization and pattern diversity," *IEEE Trans. Antennas Propag.*, vol. 67, no. 8, pp. 5145–5153, Aug. 2019.

[11] A.-K.-S. O. Hassan, H. L. Abdel-Malek, A. S. A. Mohamed, T. M. Abuelfadl, and A. E. Elqenawy, "Statistical design centering of RF cavity linear accelerator via non-derivative trust region optimization," in *IEEE MTT-S Int. Microw. Symp. Dig.*, Aug. 2015, pp. 1–3.

[12] A. Kouassi, N. Nguyen-Trong, T. Kaufmann, S. Lallechere, P. Bonnet, and C. Fumeaux, "Reliability-aware optimization of a wideband antenna," *IEEE Trans. Antennas Propag.*, vol. 64, no. 2, pp. 450–460, Feb. 2016.

[13] J. Wang, X.-S. Yang, and B.-Z. Wang, "Efficient gradient-based optimisation of pixel antenna with large-scale connections," *IET Microw., Antennas Propag.*, vol. 12, no. 3, pp. 385–389, Feb. 2018.

[14] A. Pietrenko-Dabrowska and S. Koziel, "Computationally-efficient design optimisation of antennas by accelerated gradient search with sensitivity and design change monitoring," *IET Microw., Antennas Propag.*, vol. 14, no. 2, pp. 165–170, 2020.
[15] S. Koziel and A. Pietrenko-Dabrowska, "Reduced-cost design closure of antennas by means of gradient search with restricted sensitivity update," *Metrol. Meas. Syst.*, vol. 26, no. 4, pp. 595–605, 2019.
[16] A. Darvish and A. Ebrahimzadeh, "Improved fruit-fly optimization algorithm and its applications in antenna arrays synthesis," *IEEE Trans. Antennas Propag.*, vol. 66, no. 4, pp. 1756–1766, Apr. 2018.
[17] J. Joung, "Machine learning-based antenna selection in wireless communications," *IEEE Commun. Lett.*, vol. 20, no. 11, pp. 2241–2244, Nov. 2016.
[18] S. Mishra, R. N. Yadav, and R. P. Singh, "Directivity estimations for short dipole antenna arrays using radial basis function neural networks," *IEEE Antennas Wireless Propag. Lett.*, vol. 14, pp. 1219–1222, 2015.
[19] I. A. Baratta, C. B. de Andrade, R. R. de Assis, and E. J. Silva, "Infinitesimal dipole model using space mapping optimization for antenna placement," *IEEE Antennas Wireless Propag. Lett.*, vol. 17, no. 1, pp. 17–20, Jan. 2018.
[20] S. Koziel, "Fast simulation-driven antenna design using response-feature surrogates," *Int. J. RF Microw. Comput.-Aided Eng.*, vol. 25, no. 5, pp. 394–402, Jun. 2015.
[21] A. Maalik, R. Rojas-Teran, and R. J. Burkholder, "Design curves of a substrate-backed printed-dipole in an infinite-array environment and a novel reflectarray unit-cell design example," in *Proc. IEEE/ACES Int. Conf. Wireless Inf. Technol. Syst. (ICWITS) Appl. Comput. Electromagn. (ACES)*, Mar. 2016, pp. 1–2.
[22] S. Koziel and A. Bekasiewicz, "Inverse surrogate modeling for low-cost geometry scaling of microwave and antenna structures," *Eng. Comput.*, vol. 33, no. 4, pp. 1095–1113, Jun. 2016.
[23] S. Koziel and A. Bekasiewicz, "Expedited geometry scaling of compact microwave passives by means of inverse surrogate modeling," *IEEE Trans. Microw. Theory Techn.*, vol. 63, no. 12, pp. 4019–4026, Dec. 2015.
[24] S. Koziel, A. Bekasiewicz, and L. Leifsson, "Rapid EM-driven antenna dimension scaling through inverse modeling," *IEEE Antennas Wireless Propag. Lett.*, vol. 15, pp. 714–717, 2016.
[25] S. Koziel and A. Bekasiewicz, "Fast redesign and geometry scaling of multiband antennas using inverse surrogate modeling techniques," *Int. J. Numer. Model., Electron. Netw., Devices Fields*, vol. 31, no. 3, p. e2287, May 2018.
[26] Y.-C. Chen, S.-Y. Chen, and P. Hsu, "Dual-band slot dipole antenna fed by a coplanar waveguide," in *Proc. IEEE Antennas Propag. Soc. Int. Symp.*, 2006, pp. 3589–3592.
[27] *CST Microwave Studio*, CST AG, Darmstadt, Germany, 2013.
[28] C. S. Voon, K. H. Yeap, K. C. Lai, C. K. Seah, and H. Nisar, "A compact double-psi-shaped dual band patch antenna for WLAN/LTE applications," *Microw. Opt. Technol. Lett.*, vol. 60, no. 5, pp. 1271–1275, 2018.
[29] D. M. Pozar, *Microwave Engineering*, 4th ed. Hoboken, NJ, USA: Wiley, 2012.

SLAWOMIR KOZIEL (Senior Member, IEEE) received the M.Sc. and Ph.D. degrees in electronic engineering from the Gdansk University of Technology, Poland, in 1995 and 2000, respectively, and the M.Sc. degrees in theoretical physics and in mathematics and the Ph.D. degree in mathematics from the University of Gdansk, Poland, in 2000, 2002, and 2003, respectively. He is currently a Professor with the School of Science and Engineering, Reykjavik University, Iceland. His research interests include CAD and modeling of microwave and antenna structures, simulation-driven design, surrogate-based optimization, space mapping, circuit theory, analog signal processing, evolutionary computation, and numerical analysis.

ADRIAN BEKASIEWICZ (Senior Member, IEEE) received the M.Sc., Ph.D., and D.Sc. (higher doctorate) degrees in electronic engineering from the Gdansk University of Technology, Poland, in 2011, 2016, and 2020, respectively. He is currently an Associate Professor with the Gdansk University of Technology, Poland. His research interests include EM-driven design and modeling of microwave/antenna structures, multiobjective optimization, metaheuristic algorithms, inverse modeling methogologies, as well as development of compact antennas with unconventional topologies, and miniaturization of microwave/RF components.